Int. J. Electrochem. Sci., 5 **(2010)** 531 - 546

International Journal of
ELECTROCHEMICAL
SCIENCE
www.electrochemsci.org

Novel Carbon Nanotube Paste Electrode for Simultaneous Determination of Norepinephrine, Uric Acid and D-Penicillamine

Mohammad Mazloum-Ardakani[1,*], *Hadi Beitollahi*[1], *Bahram Ganjipour*[2], *Hossein Naeimi*[3]

[1] Department of Chemistry, Faculty of Science, Yazd University, Yazd, 89195-741, I.R. Iran
[2] Institute of Nanotechnology, University of Kashan, Kashan, 87317, I.R. Iran
[3] Department of Organic Chemistry, Faculty of Chemistry, University of Kashan, Kashan, 87317, I.R. Iran
[*]E-mail: mazloum@yazduni.ac.ir

Received: 3 March 2010 / *Accepted:* 15 April 2010 / *Published:* 30 April 2010

The electro-oxidation of norepinephrine (NE), uric acid (UA), D-penicillamine (D-PA) and their mixture by modified carbon nanotube paste electrode of 2, 2'-[1, 2-ethanediylbis (nitriloethylidyne)]-bis-hydroquinone (EBNBH) has been studied using cyclic voltammetry, chronoamperometry and differential pulse voltammetry. In the mixture containing of NE, UA and D-PA, the three compounds can well separate from each other at the scan rate of 30 mVs^{-1} with potential differences of 190, 250 and 440 mV between NE - UA, UA – D-PA and NE – D-PA respectively, which was large enough to determine NE, UA and D-PA individually and simultaneously. Linear calibration plots were obtained over the concentration ranges of 0.1-1100.0 μM, 10.0-800.0 μM and 15.0-700.0 μM for NE, UA and D-PA respectively. The diffusion coefficient ($D = 4.54\times10^{-6}$ cm^2 s^{-1}), and the kinetic parameters such as electron transfer coefficient, ($\alpha = 0.41$) and heterogenous rate constant, ($k' = 1.3 \times10^{-3}$ cm s^{-1}) for NE were also determined using electrochemical approaches. The results were explained using the theory of electrocatalytic reactions at chemically modified electrodes. Further investigations of the modified carbon nanotube paste electrode show reproducible behavior and high level of stability.

Keywords: Carbon nanotube, Norepinephrine, Uric acid, D-penicillamine, Modified electrode

1. INTRODUCTION

Carbon nanotubes (CNTs) have attracted much attention during the past decade [1], due to their unique mechanical, chemical and electrical properties. CNTs with diameters in the range of 5–40 nm and up to several microns in length can now be produced in macro quantities. According to their atomic structure, CNTs behave electrically as a metal or as a semiconductor [2, 3]. They have many

significant properties and can be used as attractive novel materials in electrochemical fields [4-6]. The subtle electronic properties suggest that CNTs should have the ability to mediate electron transfer reactions with electroactive species in solution when used as an electrode. The reactivities of CNTs in solution have been demonstrated [7], resulting in specific reactive (oxidative) sites on the CNTs surfaces. Thus, an important application of CNTs is that they can be used as the electrode material in CNT paste electrodes or CNT modified glassy carbon electrodes [8, 9] to investigate the electrochemical properties of biomolecules. Recent studies have demonstrated improved electrochemical behavior of epinephrine [10], hydrazine [11], morin [12] and morphine [9] at CNT modified electrodes. The modified electrodes, in contrast with metallic electrodes, present the great advantage of possessing a large number of reactive sites and offer the possibility of being designed with particular redox active sites [13]. Another important advantage, concerning the application for the development of biosensors, is that the electroactive films can be used to entrap different biomolecules at the electrode surface [14].

NE is a very important catecholamine neurotransmitter in the mammalian central nervous system and is often monitored electrochemically in vivo with microfiber electrodes. The oxidation of this compound is interesting, and this process occurs in the human body. Catecholamine drugs are also used to treat hypertension, bronchial asthma, organic heart disease and are used in cardiac surgery and myocardial infarction. An understanding of the electrochemical reactions of NE is necessary to develop a method for studying its physiological function, and to aid diagnosis of some diseases, because in clinical medicine it is often desirable to develop an electroanalytical method to study electron transfer processes. Numerous observations on electrochemical behavior of NE and its analogs such as epinephrine have been made in many research groups [15-18].

UA, the end metabolic product of purine through the liver, is present in blood and urine. Monitoring UA in the blood or urine is important because it can be used as a powerful indicator for an early warning sign of kidney diseases. Abnormal UA level in a human body could be caused by several diseases such as gout, hyperuricemia, Lesch-Nyan syndrome, cardiovascular and chronic renal disease [17]. Furthermore, other diseases such as leukemia and pneumonia are also related with the urate levels. Various electrochemical methods have been employed to monitor the level of UA [19-22]. The advantages of electrochemical technique for determining UA are its high sensitivity, low cost and less time consumption.

D-PA is a pharmaceutically important thiol compound frequently used as a medicinal agent against a number of diseases such as rheumatoid arthritis, cystinuria, liver disease or certain skin conditions, heavy metal poisoning and Wilson's disease, a genetic disease that results in excessive copper deposits in the body tissues [23]. Increasing the amount of D-PA can cause rashes early in treatment. It can also cause loss of appetite, nausea, abdominal pain, loss of the sense of taste, bone narrow suppression and serious kidney disease [24]. Several methods have been proposed for the determination of D-PA including high performance liquid chromatography with pre or post column derivatization, calorimetry, fluorometry, spectrophotometric chemiluminescence, capillary electrophoresis and NMR spectrometry [25]. Electrochemical methods are an alternative for the D-PA determination because they are cheap, simple, fast and sensitive [26].

Recently, modified carbon paste electrodes have been studied by our research group in the fields of electrochemical sensors [27-29]. With the above in mind, in this paper we described initially the preparation and suitability of a 2, 2´-[1, 2-ethanediylbis (nitriloethylidyne)]-bis-hydroquinone modified carbon nanotube paste electrode (EBNBHCNPE) as a new electrode in the electrocatalysis and determination of NE in an aqueous buffer solution, then we evaluated the analytical performance of the modified electrode in quantification of NE in the presence of UA and D-PA.

2. MATERIALS AND METHODS

2.1. Apparatus and chemicals

Electrochemical experiments were carried out using a computerized potentiostat/galvanostat (Autolab model PGSTAT302 N, Eco Chemie B. V. A). The experimental conditions were controlled with General Purpose Electrochemical System (GPES) software. A conventional three electrode cell was used at 25 ± 1°C. An Ag / AgCl / KCl 3.0 M electrode, a platinum wire, and an EBNBHCNPE were used as reference, auxiliary and working electrodes, respectively. A Metrohm 691 pH / ion meter was also used for pH measurements.

The NE injection solution (specified content of NE is 1.0 mg mL^{-1}) was diluted to 250.0 mL with water; different volume solution was transferred into each of series of 10.0 mL volumetric flasks and diluted to the mark with phosphate buffer. An aliquot of 10.0 mL of this test solution was placed in the electrochemical cell.

All solutions were freshly prepared with twice distilled water. NE, UA and reagents were analytical grade from Merck. D-PA was from Fluka. 2, 2´-[1, 2-ethanediylbis (nitriloethylidyne)]-bis-hydroquinone (EBNBH) was synthesized in our laboratory as reported previously [9]. Graphite fine powder (Merck) and paraffin oil (DC 350, Merck, density=0.88 g cm^{-3}) were used as binding agents for the graphite pastes. The buffer solutions were prepared from orthophosphoric acid and its salts in the pH range 2.0-11.0.

2.2. Synthesis of carbon nanotubes

The nanotubes were grown by chemical vapor deposition. Several transition metal catalysts have been shown to be active for generation of carbon nanotubes [30]. Among the various formulations that we have investigated, Co–Fe silica (MCM41-96) catalyst containing 2.5 wt % total metals and a Co: Fe molar ratio of 1:1 exhibited the highest selectivity towards double wall carbon nanotubes (DWCNTs). This catalyst was prepared from methanol solutions of cobalt acetate and iron acetate, activated at 300°C for 30 min under a 500 mL/min of Ar flow in a quartz tube [31]. For the production of nanotubes, 100–500 mg of activated catalyst was placed in a horizontal quartz tubular reactor, heated in H_2 to 500°C, and then in He to 900°C. The quartz tube is pumped out during the CCVD (catalytic chemical vapor deposition) process. Methane was introduced at (900°C) for 20 min. The flow of methane was set at 10 standard cubic centimeters per minute (sccm) and the hydrogen and

helium flow were kept constant at 90 sccm throughout the heating and deposition cycles. The diameter, length, purity and surface area of DWCNTs were ~2.5 nm (outer diameter of DWCNTs is in the range of 1.52–3.54 nm), 5-15 μm, 90%, 97 m^2/g (roughly), respectively.

2.3. Preparation of the electrode

Carbon nanotube paste electrodes were prepared by dissolve 0.01 g of EBNBH in CH_3Cl and hand mixing with 89-times its weight of graphite powder and 10-times its weight of carbon nanotube with a mortar and pestle. Paraffin were added to the above mixture using a 5 mL syringe and mixed for 20 min until a uniformly-wetted paste was obtained. The paste was then packed into the end of a glass tube (ca. 2 mm i.d. and 10 cm long). A copper wire inserted into the carbon paste provided the electrical contact. When necessary, a new surface was obtained by pushing an excess of paste out of the tube and then polished with a weighing paper.

Unmodified carbon paste was prepared in the same way without adding EBNBH and carbon nanotube to the mixture and was used for comparison purposes.

3. RESULTS AND DISCUSSION

3.1. Cyclic voltammetric investigations

The electrochemical behavior of the EBNBH at the CNT paste electrode was investigated, using cyclic voltammetry in aqueous solution. The cyclic voltammograms for the modified electrode studied at different scan rates in 0.1 M phosphate buffer with pH 7.0. Cyclic voltammogram exhibited an anodic peak at a forward scan of the potential related to the oxidation of the EBNBH to quinone form of EBNBQ. Where as at a reverse scan of the potential, a cathodic peak appears related to the reduction of quinone form EBNBQ to EBNBH. A pair of reversible peaks observed at E_{pa}=0.180 V and E_{pc}= 0.115 V vs. Ag/AgCl. Formal potential ($E^{0'}$) and ΔE_p were 0.148 V vs. Ag/AgCl and 0.065 V, respectively. The peak separation potential, ΔE_p (=E_{pa} - E_{pc}), is greater than the (59/n) mV expected for a reversible system. Therefore EBNBH / EBNBQ redox couple in EBNBHCNPE shows a quasi reversible behavior in an aqueous medium.

Fig. 1A show anodic and cathodic peak currents (I_p) values were linearity dependent on υ (at different scan rates, in the range 10-1000 mV s^{-1}). A linear correlation was obtained between peak currents and the scan rate indicate that the nature of redox process is diffusionless controlled. Magnitudes of peak potentials (E_{pa} and E_{pc}) as a function of the potential scan rate are shown in the Fig. 1B. The surface coverage can be evaluated by adopting the method used by Bard [32]. The values for the surface concentration of EBNBH (Γ), given in mol cm^{-2} was obtained from the integrated charges (Q) of the anodic peak as follows:

$$\Gamma_{EBNBH} = Q/nFA \quad (1)$$

where Q is the charge obtained by integrating charges from the EBNBH anodic peak area corrected for the baseline, and could be easily observed from cyclic voltammograms; n is the number of electrons exchanged per reactant molecule (n = 2). The surface concentration of EBNBH was 2.5× 10^{-10} mol cm^{-2}.

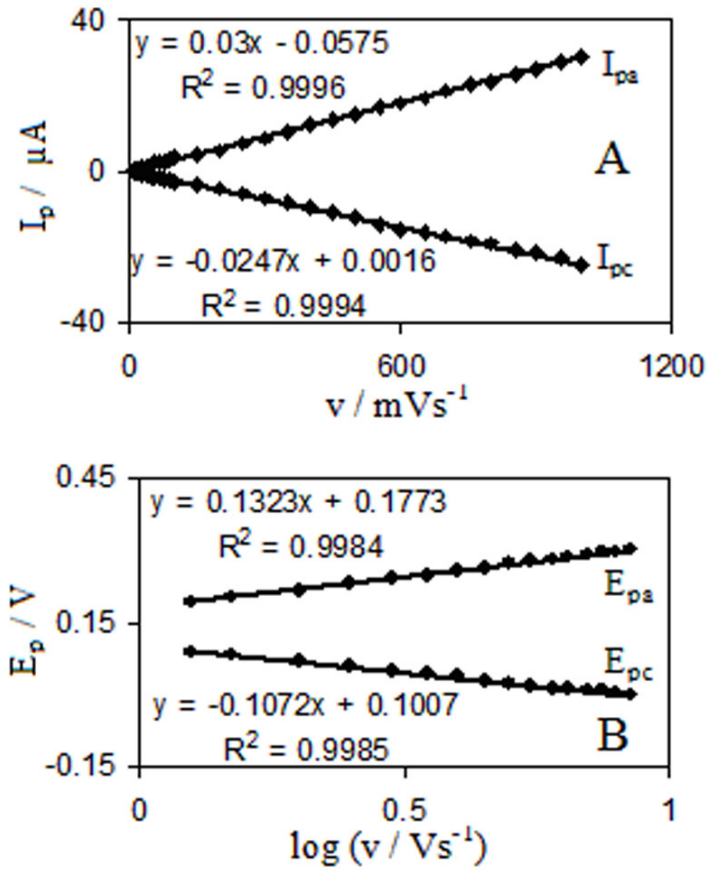

Figure 1. (A) The plot of anodic (a) and cathodic (b) peak currents of EBNBHCNPE vs. ν from the cyclic voltammograms of EBNBHCNPE in 0.1 M phosphate buffer solution (PBS) (pH 7.0), at various scan rates (data points from left to right): 10, 20, 50, 100, 200, 300, 400, 500, 600, 700, 800, 900 and 1000 mVs^{-1}. (B) Variation of E_{pa} and E_{pc} versus the logarithm of the high scan rates.

Laviron derived general expressions for the linear potential sweep voltammetric response for the case of surface-confined electroactive species with a concentration small enough [33]:

$$E_{pc}=E^{\circ}+A \ln [(1-\alpha)/m] \quad (2)$$

$$E_{pa}=E^{\circ}+B \ln [\alpha/m] \quad (3)$$

For $E_{pa} - E_{pc}=\Delta E_p > 200/n$ mV:

$$\log k_s=\alpha \log (1-\alpha) + (1-\alpha) \log \alpha - \log (RT/nF\nu) - \alpha n_{\alpha} F\Delta E_p(1-\alpha) /2.3RT \quad (4)$$

Where $A=RT/(1-\alpha)\,nF$, $B=RT/\alpha nF$ and $m=(RT/F)(k_s/n_\alpha)$; other terms have their usual significance.

From these expressions it is possible to determine the transfer coefficient (α) by measuring the variation of the peak potentials with scan rate (ν) as well as the apparent charge transfer rate constant (k_s) for electron transfer between the electrode and the surface-confined layer of EBNBH. A graph of E_p= f (log ν) yields two straight lines with slopes equal to $-2.3RT/\alpha nF$ and $2.3RT/(1-\alpha)\,nF$ for the cathodic and anodic peaks, respectively. We have found that for scan rates above 1000 mVs^{-1}, the values of $\Delta E= (E_{pa}- E_{pc})$ were proportional to the logarithm of scan rate as was indicated by Laviron. The plots are shown in of Fig. 1B. Using such plot and Eq. (4), the values of α and k_s were 0.55 and 8.89 s^{-1}, respectively, for the EBNBHCNPE in the presence of 0.1 M phosphate buffer.

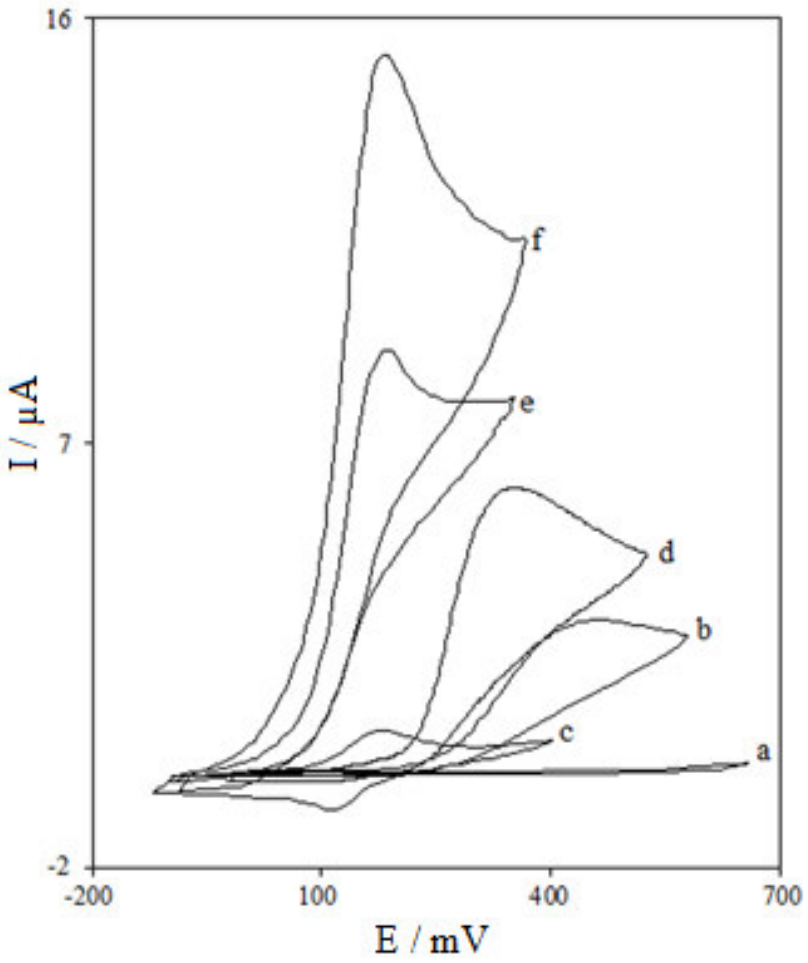

Figure 2. Cyclic voltammograms of (a) CPE in 0.1M phosphate buffer solution (pH 7.0) at scan rate 30 mV s^{-1} and (b) as (a) + 1.0 mM NE; (c) as (a) and (d) as (b) at the surface of EBNBHCNPE and CNPE respectively. Also, (e) and (f) as (b) at the surface of EBNBHCPE and EBNBHCNPE.

Table 1. Comparison of the efficiency of some modified electrodes used in the electrocatalysis of NE

Substrate	Modifier	Method	pH	Peak potential shift (mV)	Scan rate (mV/s)	Limit of detection (M)	Dynamic range (M)	Reference
Glassy Carbon Electrode	Nickel(II) Complex	Voltammetry	7.4	_	100	7.7×10^{-9}	1.0×10^{-7} - 1.0×10^{-5}	15
Glassy Carbon Electrode	Poly(Cresol Red)	Voltammetry	3.0	110	100	2.0×10^{-7}	3.0×10^{-6} - 3.0×10^{-5}	17
Glassy Carbon Electrode	Gold Nanoparticles	Voltammetry	7.4	200	50	2.0×10^{-8}	5.0×10^{-7} - 8.0×10^{-5}	36
Glassy Carbon Electrode	Poly(2,4,6-trimethylpyridine)	Voltammetry	7.4	-	100	8.0×10^{-6}	5.0×10^{-3} - 1.0×10^{-1}	37
Carbon Nanotube Paste Electrode	2, 2'-[1, 2 Ethanediylbis (nitriloethylidyne)]-bis hydroquinone	Voltammetry	7.0	270	30	8.2×10^{-8}	1.0×10^{-7}– 1.1×10^{-3}	This work

3.2. Electrocatalytic oxidation of NE at the surface of EBNBHCNPE

Fig. 2 demonstrates the cyclic voltammetric responses from the electrochemical oxidation of 1.0 mM NE at EBNBHCNPE (curve f), EBNBH modified carbon paste electrode (EBNBHCPE) (curve e), carbon nanotube paste electrode (CNPE) (curve d) and bare CPE (curve a). As can be seen, the anodic peak potential for the oxidation of NE at EBNBHCNPE (curve f) and EBNBHCPE (curve e) is about 180 mV, while at the CNPE (curve d) peak potential is about 350 mV, and at the bare CPE peak potential is about 450 mV for NE (curve b). From these results it is concluded that the best electrocatalytic effect for NE oxidation is observed at EBNBHCNPE (curve f). Moreover, the results show that the peak potential of NE oxidation at EBNBHCNPE (curve f) shifted by about 170 and 270 mV toward the negative values compared with that at a CNPE (curve d) and bare CPE (curve b), respectively. Similarly, when we compared the oxidation of NE at the EBNBHCPE (curve e) and EBNBHCNPE (curve f) there is a dramatic enhancement of the anodic peak current at EBNBHCNPE relative to the value obtained at the EBNBHCPE. In the other words, the data obtained clearly show that the combination of carbon nanotube and mediator (EBNBH) definitely improve the characteristics of NE oxidation. The EBNBHCNPE in 0.1M phosphate buffer (pH 7.0), without NE in solution, exhibits a well-behaved redox reaction (curve c). Upon the addition of 1.0 mM NE, there is a dramatic enhancement of the anodic peak current (curve f), which indicates a strong electrocatalytic effect [32].

This value is comparable with values reported by other research groups for electrocatalytic oxidation of NE at the surface of chemically modified electrodes by other mediators (Table 1).

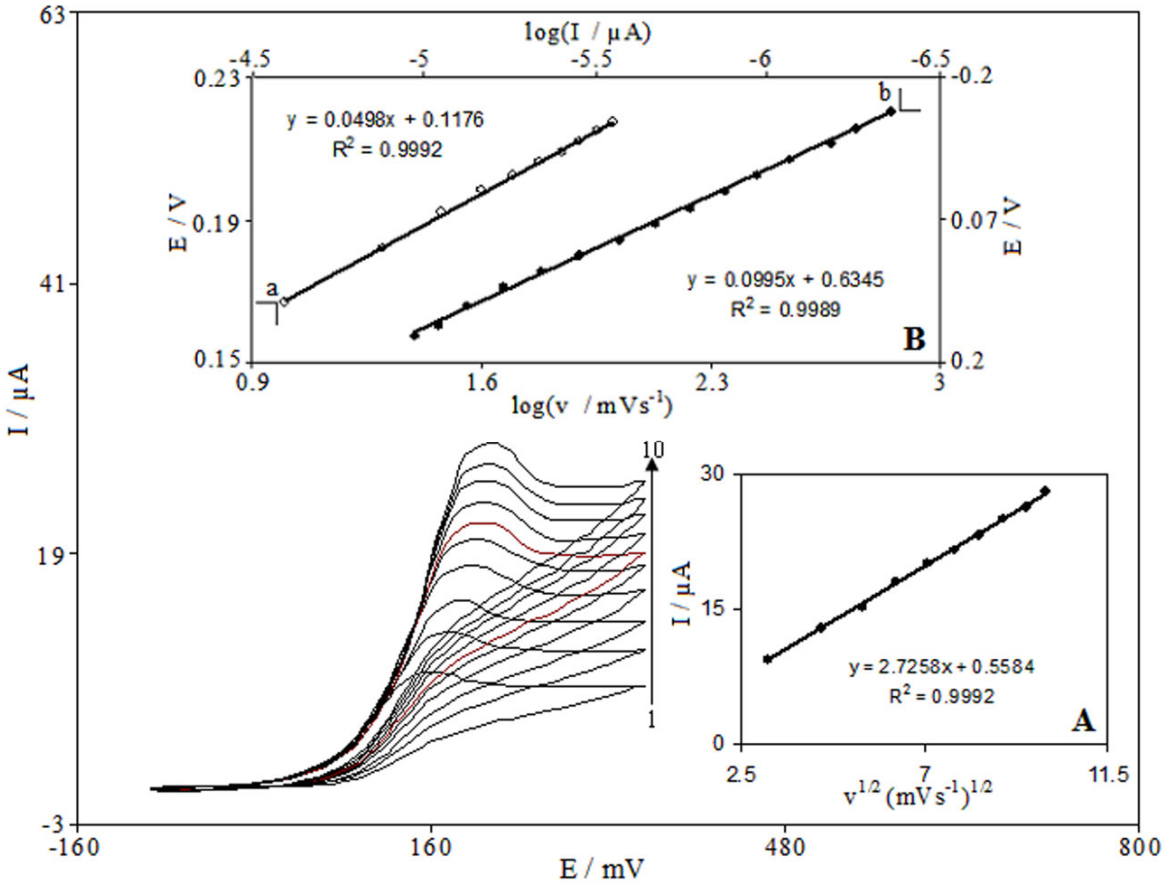

Figure 3. Cyclic voltammograms of the EBNBHCNPE in the presence of 1.0 mM NE at various scan rates; The numbers 1-10 correspond to 10, 20, 30, 40, 50, 60, 70, 80, 90 and 100 mVs^{-1} scan rates, respectively Insets:(A) The variation of the anodic peak currents vs. $v^{1/2}$. (B) Curve a, variation of the anodic peak potential vs. log *v*. and curve b, Tafel plot derived from the rising part of voltammogram recorded at a scan rate 30 mVs^{-1}.

Information about the catalytic mechanism can be obtained from the cyclic voltammograms of NE solution at different scan rates. Fig. 3 shows the cyclic voltammograms of a EBNBHCNPE at various scan rates obtained in 0.1 M phosphate buffer solution (pH 7.0) containing 1.0 mM NE. The anodic oxidation current of NE is proportional to the square root of the scan rate (Fig. 3, inset A) indicating that at sufficiently positive potential the reaction is controlled by NE diffusion.

From the slope of E_p vs. log ν as is shown in Fig. 3 (inset B), the Tafel slope can also be obtained from the following equation [34]:

$$E_p = (b/2) \log \nu + \text{constant} \quad (5)$$

The slope of E_p vs. log ν plot is b/2, where b indicates the Tafel slope. The slope of E_p vs. log ν plot is $\partial E_p / \partial (\log \nu)$ was found to be 49.8 mV in this work (Fig. 3, inset B, curve a), so, b = 2 × 49.8 = 99.6 mV. The value of Tafel slope indicates that a one-electron transfer process is the rate limiting step assuming a transfer coefficient of α about 0.41. Fig. 3 inset B, curve b, shows a Tafel plot that was drawn from data of the rising part of the current–voltage curve recorded at a scan rate of 30 mVs^{-1}. This part of voltammogram, known as Tafel region, is affected by electron transfer kinetics between substrate (NE) and surface confined EBNBH. In this condition, the number of electron involved in the rate determining step can be estimated from the slope of Tafel plot. A slope 99.5 $mVdecade^{-1}$ is obtained indicating a one electron transfer to be rate limiting assuming a transfer coefficient of α = 0.41.

The peak current for the anodic oxidation is proportional to the square root of scan rate (Fig. 3, inset A), which indicate that the reaction involves mass transport. Using the slope of this plot and according to the following equation for a totally irreversible diffusion-controlled process [32]:

$$I_p = 2.99\times10^5\ n\ [(1-\alpha)n_\alpha]^{1/2}\ A\ C^*\ D^{1/2}\ \nu^{1/2} \qquad (6)$$

and considering $(1-\alpha)n_\alpha$=0.59, it is estimated that the total number of electrons involved in the anodic oxidation of NE is n = 1.8 ~ 2.

3.3. Chronoamperometric measurements

The catalytic oxidation of NE by EBNBHCNPE was studied by chronoamperometry. Fig. 4 shows chronoamperograms that were obtained for a series of NE solutions with various concentrations at EBNBHCNPE. The results show that an increase in concentration of NE was accompanied by an increase in anodic current obtained for a potential of 250 mV vs. Ag/AgCl. In chronoamperometric studies, we have determined the diffusion coefficient of NE for an EBNBHCNPE. For an electroactive material (NE in this case) with a diffusion coefficient of D, the current for the electrochemical reaction (at a mass transport limited rate) is described by the Cottrell equation [32]:

$$I = nFAD^{1/2}C_b\pi^{-1/2}t^{-1/2} \qquad (7)$$

Where D and C_b are the diffusion coefficient ($cm^2\ s^{-1}$) and the bulk concentration (mol cm^{-3}) respectively. The experimental plots of I versus $t^{-1/2}$, with the best fit for different concentrations of NE were employed. The slopes of the resulting straight lines were plotted versus the NE concentrations (Fig. 4 inset A). The diffusion coefficient was calculated as $4.54\times10^{-6}\ cm^2\ s^{-1}$ for NE.

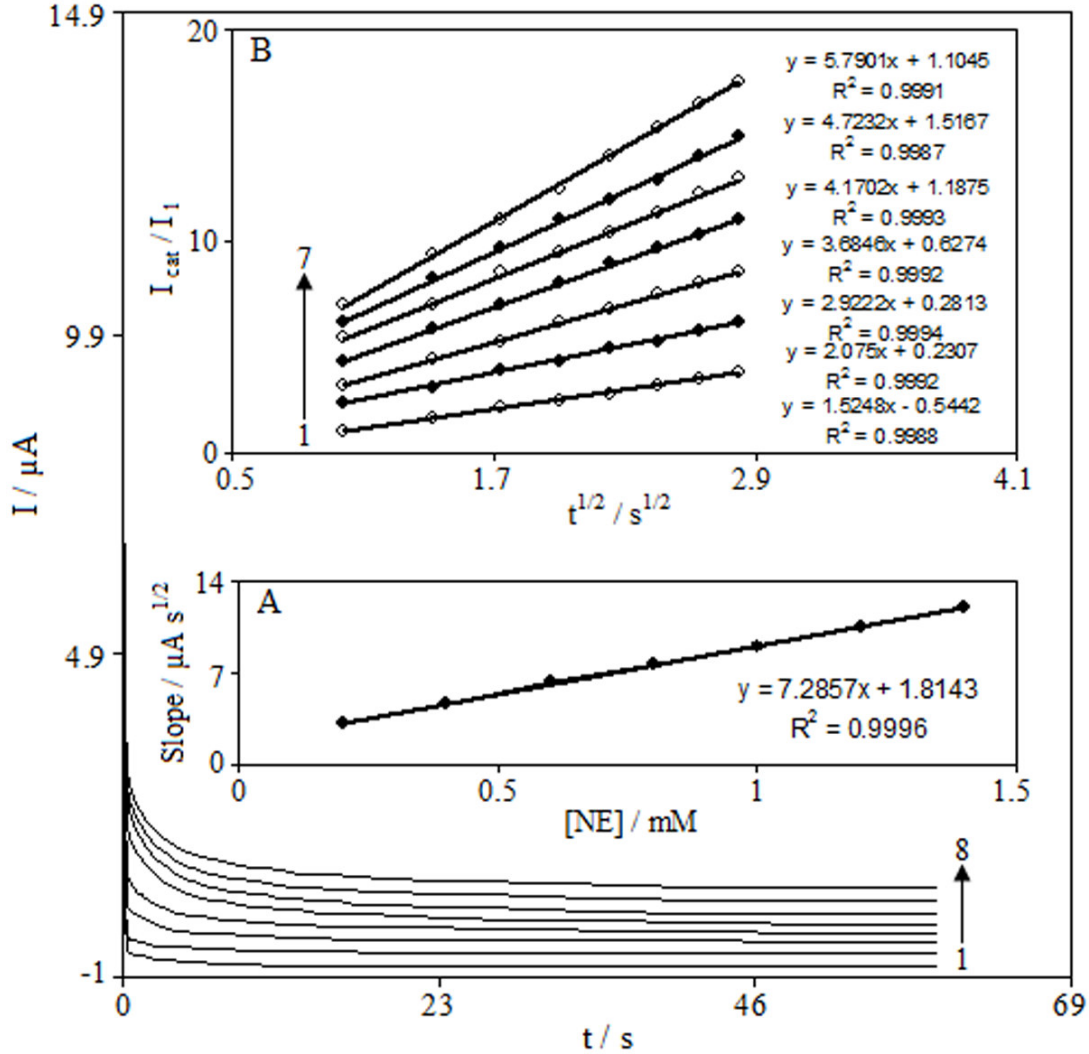

Figure 4. Chronoamperograms obtained at EBNBHCNPE in 0.1 M phosphate buffer solution (pH 7.0) for different concentration of NE. The numbers 1-8 correspond to 0.0, 0.2, 0.4, 0.6, 0.8, 1.0, 1.2 and 1.4 mM of NE. Inset: (A) plot of the slope of the straight lines against the NE concentration. (B) Dependence of I_{cat}/I_l on $t^{1/2}$ derived from the data of chronoamprograms.

Also chronoamperometry can be used to estimate of the catalytic rate constant, k, for the reaction between NE and the EBNBHCNPE according to the method of Galus [35]:

$$I_C / I_L = \gamma^{1/2}[\pi^{1/2} \operatorname{erf}(\gamma^{1/2}) + \exp(-\gamma) / \gamma^{1/2}] \quad (8)$$

Where I_C is the catalytic current of NE at the EBNBHCNPE, I_L the limited current in the absence of NE and $\gamma = kC_bt$ (C_b is the bulk concentration of NE) is the argument of the error function. In the cases where γ exceeds 2 the error function is almost equal to 1 and therefore the above equation can be reduced to:

$$I_C / I_L = \pi^{1/2} \gamma^{1/2} = \pi^{1/2} (kC_bt)^{1/2} \quad (9)$$

where t is the time elapsed (s). The above equation can be used to calculate the rate constant of the catalytic process k. Based on the slope of the I_C / I_L versus $t^{1/2}$ plot; k can be obtained for a given NE concentration. Such plots obtained from the chronoamperograms are shown in Fig. 4 inset B. From the values of the slopes an average value of k was found to be k= 5.19×10^3 M^{-1} s^{-1}. The value of k explains as well as the sharp feature of the catalytic peak observed for catalytic oxidation of NE at the surface of EBNBHCNPE. Finally, the heterogeneous rate constant of catalytic reaction was calculated as k´= 1.3×10^{-3}cm s^{-1}.

3.4. Differential pulse voltammetry investigations

Differential pulse voltammetry (DPV) has the advantage of an increase in sensitivity and better characteristics for analytical applications. DPVs for the oxidation of different concentrations of NE at the EBNBHCNPE were obtained (Not shown). Voltammograms clearly show that the plot of peak current versus NE concentration is constituted of two linear segments with different slopes (slope: 0.1555 $\mu A.\mu M^{-1}$ for first linear segment and 0.0151 $\mu A.\mu M^{-1}$ for second linear segment), corresponding to two different ranges of substrate concentration (0.1 to 35.0 μM for first linear segment and 35.0 to 1100.0 μM for second linear segment). The decrease of sensitivity (slope) in the second linear range is likely to be due to kinetic limitation. The detection limit (3σ) for NE in the lower range region was found to be 0.082 μM. In Table 1 the response characteristics of the proposed electrode are compared with values reported by other research groups.

3.5. Simultaneous determination of NE, UA and D-PA at EBNBHCNPE

One of the main objectives of this study was the development of a modified electrode capable of the electrocatalytic oxidation of NE and separation of the electrochemical responses of NE, UA and D-PA. Since differential pulse voltammetry, DPV has a much higher current sensitivity and better resolution than cyclic voltammetry, it was used to simultaneous determination of NE, UA and D-PA. In addition, the charging current contribution to the background current, which is a limiting factor in the analytical determination, is negligible in DPV mode. Using EBNBHCNPE as the working electrode the analytical experiments were carried out either by varying the UA or the D-PA concentrations in the presence of 100.0 μM and 425.0 μM NE in 0.1 M phosphate buffer (pH 7.0) respectively. Fig. 5 shows DPVs obtained with increasing concentrations of UA in the presence of 100.0 μM NE and the inset shows the plot of peak current versus UA concentration. Fig. 5 B shows DPVs obtained with increasing concentrations of D-PA in the presence of 425.0 μM NE and the inset shows the plot of peak current versus D-PA concentration. As shown in Fig. 5A, an increase in the peak current of UA is observed with increasing UA concentration and the voltammetric peak of NE is almost unchanged during the oxidation of UA. Fig. 5B shows that the various concentrations of D-PA in the presence of 425.0 μM NE exhibit excellent DPV responses with the response to NE remaining almost constant. It can also be noted from these results that the responses to NE, UA and D-PA at the EBNBHCNPE are relatively independent. The utilization of the EBNBHCNPE for the simultaneous

determination of NE, UA and D-PA was demonstrated by simultaneously changing the concentrations of NE, UA and D-PA. The DP voltammetric results show that the simultaneous determination of NE, UA and D-PA with three well-distinguished anodic peaks at potentials of 100.0, 290.0 and 540.0 mV, corresponding to the oxidation of NE, UA and D-PA, respectively, is possible at the modified electrode (Fig. 6). Fig. 6 insets, A, B and C show the dependence of DPV peak currents on the concentrations of NE, UA and D-PA respectively.

It is very interesting to note that the sensitivities of the modified electrode towards NE in the absence and presence of UA and D-PA are virtually the same, which indicates the fact that the oxidation processes of NE, UA and D-PA at the EBNBHCNPE are independent and therefore simultaneous or independent measurements of the three analytes are possible without any interference. If the NE signal is affected by the UA or the D-PA, the above-mentioned slopes would be different.

3.6. The repeatability and stability of EBNBHCNPE

The electrode capability for the generation of a reproducible surface was examined by cyclic voltammetric data obtained in optimum solution pH from five separately prepared EBNBHCNPEs. The calculated RSD for various parameters accepted as the criteria for a satisfactory surface reproducibility (1-4%). This degree of reproducibility is virtually the same as that expected for the renewal or ordinary carbon paste surface. In addition, the long-term stability of the EBNBHCNPE was tested over a three-week period. When CV's were recorded after the modified electrode was stored in an atmosphere at room temperature, the peak potential for NE oxidation was unchanged and the current signals showed only less than 2.4% decrease of the initial response. The antifouling properties of modified electrode toward NE oxidation and its oxidation products were investigated by recording the cyclic voltammograms of modified electrode before and after using in the presence of NE. Cyclic voltammograms were recorded in the presence of NE after having cycled the potential for 15 cycles at a scan rate 30 mVs^{-1}. The peak potentials were unchanged to positive values and the currents decreased by less than 2.2%. Therefore, at the surface of EBNBHCNPE, not only the sensitivity increase, but the fouling effect of the analyte and its oxidation product also decreases. However we regenerated the surface of EBNBHCNPE before each experiment.

3.7. Interference study

The influence of various foreign species on the determination of 1.0×10^{-4} M NE, 6.0×10^{-5} M UA and 6.0×10^{-5} M D-PA were investigated. The tolerance limit was taken as the maximum concentration of the foreign substances, which caused an approximately ±5% relative error in the determination. The tolerated concentration of foreign substances was 1.0×10^{-1} M for Na^+, Cl^- and K^+; 6.0×10^{-2} M for Mg^{2+} and Ca^{2+}; 5.0×10^{-3} M for L-lysine, glucose, NADH, L-asparagine, glutamic acid, glycine, L-cystine, L-cysteine and acetaminophene. Also ascorbic acid, dopamine and epinephrine showed interferences.

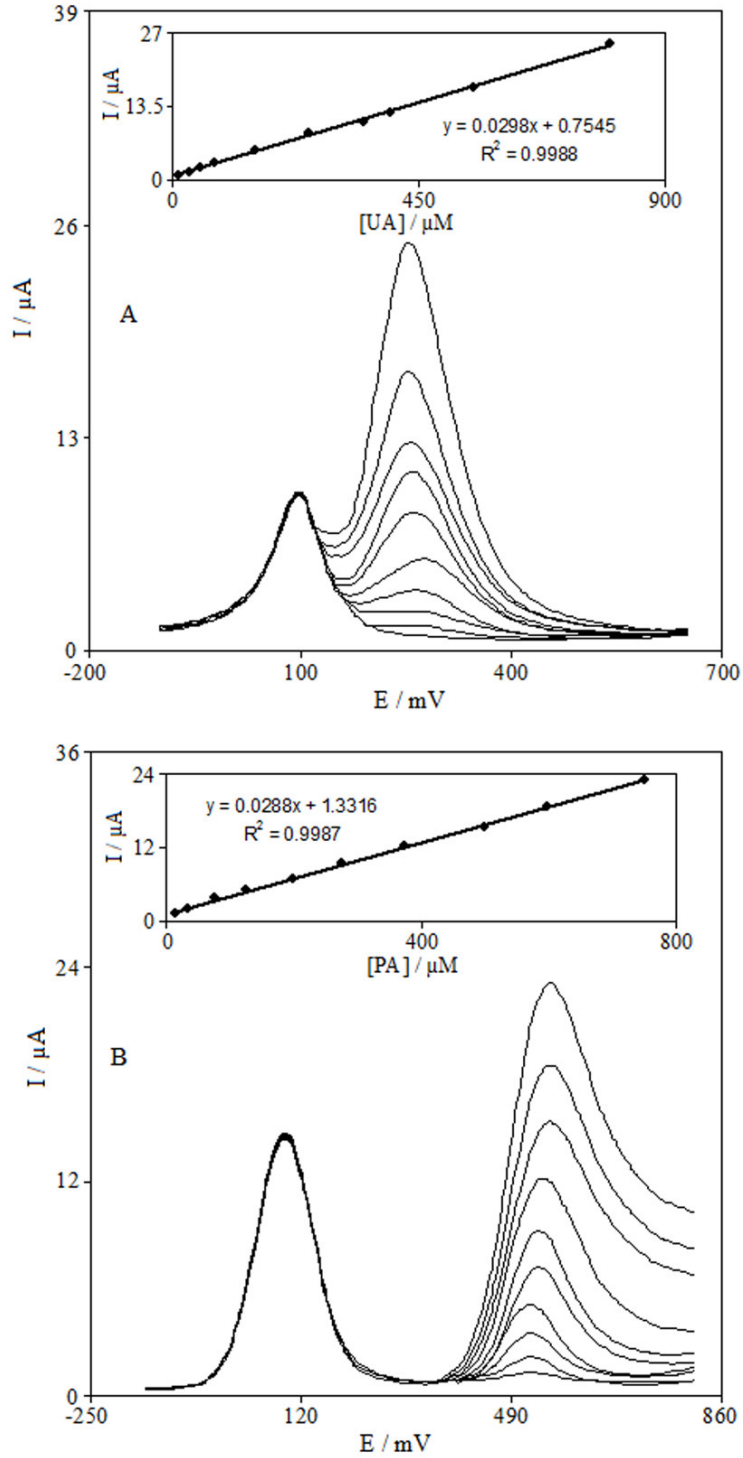

Figure 5. (A) Differential pulse voltammograms of EBNBHCNPE in 0.1 M phosphate buffer solution (pH 7.0) containing 100.0 µM NE and different concentrations of UA (from inner to outer):10.0, 30.0, 50.0, 75.0, 150.0, 250.0, 350.0, 400.0, 550.0 and 800.0 µM. Inset: plot of the electrocatalytic peak current as a function of UA concentration. (B) Differential pulse voltammograms of EBNBHCNPE in 0.1 M phosphate buffer solution (pH 7.0) containing 425.0 µM NE and different concentrations of D-PA (from inner to outer): 15.0, 35.0, 75.0, 125.0, 200.0, 275.0, 375.0, 500.0, 600.0 and 700.0 µM of D-PA. Inset: plot of the electrocatalytic peak current as a function of D-PA concentration.

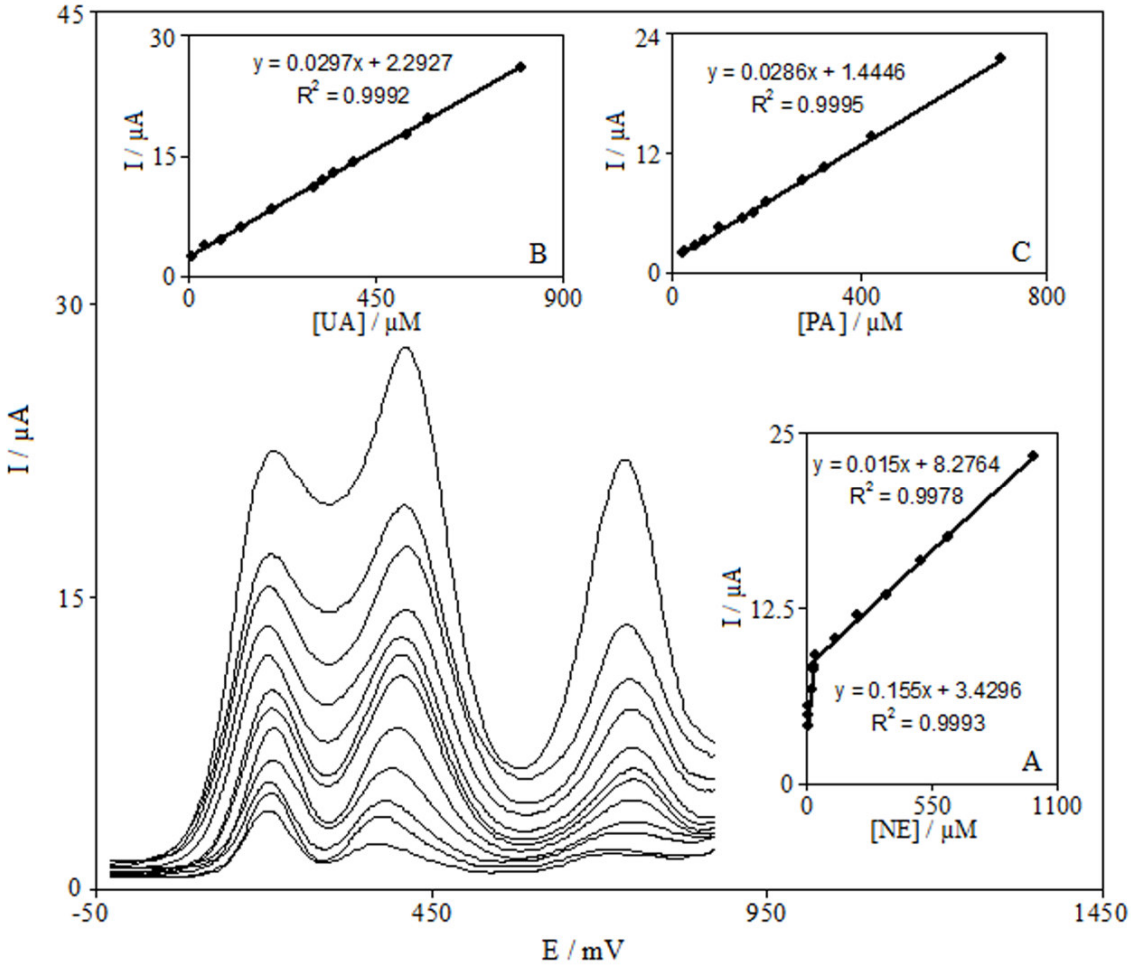

Figure 6. Differential pulse voltammograms of EBNBHCNPE in 0.1M phosphate buffer solution (pH 7.0) containing different concentrations of NE, UA and D-PA. (from inner to outer) mixed solutions of 4.0+10.0+20.0, 10.0+40.0+25.0, 13.0+80.0+50.0, 21.0+125.0+70.0, 30.0+200.0+100.0, 40.0+300.0+150.0, 125.0+325.0+175.0, 225.0+350.0+200.0, 350.0+400.0+275.0, 500.0+525.0+325.0, 625.0+575.0+425.0 and 1000.0+800.0+700.0, respectively, in which the first value is concentration of NE in µM, the second value is concentration of UA and the third value is concentration of D-PA in µM. (A) Plot of the peak currents as a function of NE concentration(in the linear range of 0.1-35.0 µM of NE; and in the linear range of 35.0-1100.0 µM of NE; (B) plot of the peak currents as a function of UA concentration and (C) plot of the peak currents as a function of D-PA concentration.

3.8. Determination of NE in NE injection

In order to assess the applicability of the proposed electrode, an attempt was made to determine NE in NE injection using the standard addition method. Samples were prepared according to section 2.1. The potentials were controlled between −0.1 and 0.4 V for cyclic scan at 30 mVs^{-1}. I_{pa} was measured at the oxidation potential of NE. The average determination results of NE in the injection were 1.02 mg mL^{-1}, which were quite corresponding to the value that was given by injection specification. This process was repeated five times and the relative standard deviation obtained was

2.3%. Different standard concentrations of NE were added to the diluted NE injection and the recoveries were between 96% and 102.4% for five measurements (Tables 2).

Table 2. Determination of NE in NE injection (n=5)

No	NE injection[a] (μM)	Found (μM)	Recovery (%)	RSD (%)
1	5.0	4.8	96.0	2.8
2	5.0	4.8	96.0	3.5
3	7.5	7.4	98.7	2.4
4	7.5	7.3	97.3	2.9
5	10.0	10.2	102.0	3.1
6	10.0	10.1	101.0	3.5
7	12.5	12.8	102.4	3.6
8	12.5	12.7	101.6	4.1

[a] From Darou Pakhsh Co. Tehran, Iran.

4. CONCLUSIONS

This work demonstrates the construction of a chemically modified carbon nanotube paste electrode by the incorporation of EBNBH as modifying species. The value of the peak separation potential obtained for the EBNBH / EBNBQ redox couple suggests that the couple can act as quasi-reversible system in the carbon nanotube paste matrix. The electrochemical behavior of the EBNBHCNPE has been studied by cyclic voltammetry and chronoamperometry in both the absence and presence of NE. The results show that the oxidation of NE is catalyzed at pH 7.0, whereas the peak potential of NE is shifted by 270 mV to a less positive potential at the surface of the EBNBHCNPE. The high current sensitivity, low detection limit and high selectivity of the EBNBHCNPE for the detection of NE prove its potential sensing applications. The EBNBHCNPE exhibits highly electrocatalytic activity to the oxidations of NE, UA and D-PA. The modified electrode displays higher selectivity in voltammetric measurements of NE, UA and D-PA in their mixture solution.

ACKNOWLEDGEMENTS
The authors wish to thank the Yazd University Research Council, the IUT Research Council and Excellence in Sensors for financial support of this research.

References

1. S. Iijima, *Nature,* 354 (1991) 56.
2. J.W.G. Wildoer, L.C. Venema, A.G. Rinzler, R.E. Smalley, C. Dekker, *Nature,* 391 (1998) 59.
3. T.W. Odom, J.L. Huang, P. Kim, C.M. Lieber, *Nature,* 391 (1998) 62.
4. H. Wang, C. Zhou, J. Liang, H. Yu, F. Peng, J. Yang, *Int. J. Electrochem. Sci.,* 3 (2008) 1258.
5. X. Chen, J.J. Zhang, J. Xuan, J.J. Zhu, *Nano Res.*, 2 (2009) 210.
6. P. Xiao, W. Wu, J. Yu, F. Zhao, *Int. J. Electrochem. Sci.,* 2 (2007) 149.

7. M. Mazloum-Ardakani, H. Beitollahi, B. Ganjipour, H. Naeimi, M. Nejati, *Bioelectrochemistry*, 75 (2009) 1.
8. H. Zhang, K. Wu1, *Microchim. Acta,* 149 (2005) 73.
9. H. Beitollahi, M. Mazloum Ardakani, H. Naeimi, B. Ganjipour, *J. Solid. State. Electrochem.,* 13 (2009) 353.
10. H. Beitollahi, M. Mazloum-Ardakani, B. Ganjipour, H. Naeimi, *Biosens. Bioelectron.,* 24 (2008) 362.
11. B. Fang, C. Zhang, W. Zhang, G. Wang, *Electrochim. Acta,* 55 (2009) 178.
12. P. Xiao, Q. Zhou, F. Xiao, F. Zhao, B. Zeng, *Int. J. Electrochem. Sci.,* 1 (2006) 228.
13. J.B. Raoof, R. Ojani, H. Beitollahi, R. Hossienzadeh, *Electroanalysis,* 18 (2006) 1193.
14. M. Mazloum-Ardakani, H. Beitollahi, M.A. Sheikh-Mohseni, H. Naeimi, N. Taghavinia, *Appl. Catal. A: Gen.,* 378 (2010) 195.
15. H. Seol, H. Jeong, S. Jeon, J. *Solid State Electrochem.,* 13 (2009) 1881.
16. M. Wei, M. Li, N. Li, Z. Gu, X. Duan, *Electrochim. Acta,* 47 (2002) 2673.
17. W. Ren, H.Q. Luo, N.B. Li, *Biosens. Bioelectron.,* 21 (2006) 1086.
18. W. Chen, X. Lin, H. Luo, L. Huang, *Electroanalysis,* 17 (2005) 941.
19. M. Mazloum Ardakani, Z.Akrami, H.Kazemian, H.R. Zare, *J. Electroanal. Chem.,* 586 (2006) 31.
20. Y. Zeng, J. Xu, K. Wu, *Microchim. Acta* 161 (2008) 249.
21. H. Tang, G.Z. Hu, S.X. Jiang, X. Liu, *J. Appl. Electrochem.* 39 (2009) 2323.
22. M. Mazloum Ardakani, A. Talebi, H. Naeimi, M. Nejati Barzoky, N. Taghavinia, *J. Solid. State. Electrochem.,* 13 (2009) 1433.
23. C. Smolarek, W.Z. Stremmel, *Gastroenterol.* 37 (1999) 293.
24. A.A.J. Torriero, E. Salinas, E.J. Marchevsky, J. Raba, J.J. Silber, *Anal. Chim. Acta,* 580 (2006) 136.
25. J. Russell, J.A. McKeown, C. Hensman, W.E. Smith, J. Reglinski, *J. Pharm. Biomed. Anal.,* 15 (1997) 1757.
26. J.B. Raoof, R. Ojani, F. Chekin, R. Hossienzadeh, *Int. J. Electrochem. Sci.,* 2 (2007) 848.
27. M. Mazloum-Ardakani, H. Rajabi, H. Beitollahi, B. B. F. Mirjalili, A. Akbari, N. Taghavinia, *Int. J. Electrochem. Sci.* 5 (2010) 147.
28. M. Mazloum-Ardakani, F. Habibollahi, H. R. Zare, H. Naeimi, M. Nejati, *J. Appl. Electrochem.* 39 (2009) 1117.
29. M. Mazloum-Ardakani, F. Habibollahi, H. R. Zare, H. Naeimi, *Int. J. Electrochem. Sci.* 3 (2008) 1236.
30. T. Sugai, H. Yoshida, T. Shimada, T. Okazaki, H. Shinohara, S. Bandow, *Nano Lett.,* 3 (2003) 769.
31. P. Ramesh, T. Okazaki, T. Sugai, J. Kimura, N. Kishi, K. Sato, Y. Ozeki, H. Shinohara, *Chem. Phys. Lett.,* 418 (2006) 408.
32. A.J. Bard, L.R. Faulkner, Electrochemical Methods, Fundamentals and Applications, Wiley, New York, 2001.
33. E. Laviron, *J. Electroanal. Chem.,* 101 (1979) 19.
34. C.P. Andrieux, J.M. Saveant, *J. Electroanal. Chem.,* 93 (1978) 163.
35. Z. Galus, Fundamentals of Electrochemical Analysis, Ellis Horwood, New York 1976.
36. L.P. Lu, S.Q. Wang, X.Q. Lin, *Anal. Chim. Acta,* 519 (2004) 161.
37. G.R. Xu, H.Y. Chang, H. Cho, W. Meng, I.K. Kang, Z.U. Bae, *Electrochim. Acta,* 49 (2004) 4069.

© 2010 by ESG (www.electrochemsci.org)